doi:10.1016/j.jmb.2007.05.041 J. Mol. Biol. (2007) 371, 447–456

JMB

Available online at www.sciencedirect.com

ScienceDirect

ELSEVIER

# Structural Basis of Phospholipase Activity of *Staphylococcus hyicus* lipase

**Jan J. W. Tiesinga, Gertie van Pouderoyen, Marco Nardini Stéphane Ransac and Bauke W. Dijkstra***

*Laboratory of Biophysical Chemistry, University of Groningen, Nijenborgh 4 9747 AG Groningen The Netherlands*

*Corresponding author

*Staphylococcus hyicus* lipase differs from other bacterial lipases in its high phospholipase $A_1$ activity. Here, we present the crystal structure of the *S. hyicus* lipase at 2.86 Å resolution. The lipase is in an open conformation, with the active site partly covered by a neighbouring molecule. Ser124, Asp314 and His355 form the catalytic triad. The substrate-binding cavity contains two large hydrophobic acyl chain-binding pockets and a shallow and more polar third pocket that is capable of binding either a (short) fatty acid or a phospholipid head-group. A model of a phospholipid bound in the active site shows that Lys295 is at hydrogen bonding distance from the substrate's phosphate group. Residues Ser356, Glu292 and Thr294 hold the lysine in position by hydrogen bonding and electrostatic interactions. These observations explain the biochemical data showing the importance of Lys295 and Ser356 for phospholipid binding and phospholipase $A_1$ activity.



*Keywords:* *Staphylococcus hyicus* lipase; phospholipase; substrate specificity; alpha/beta hydrolase fold; crystal structure

## Introduction

Lipases (glycerol ester hydrolases, EC 3.1.1.3) catalyse the hydrolysis of ester bonds in long-chain acylglycerols. The availability of large amounts of biochemical data and many crystal structures means that their catalytic mechanism, reaction selectivity and substrate specificity are very well understood.[1–4] Most lipases display interfacial activation, i.e. they show a sharp increase in activity in the presence of lipid aggregates.[5] This activity increase has been correlated with the opening of an amphipathic helical lid-domain that covers the active site in the absence of substrate aggregates.[6,7] The flexible lid-domain is attached to the core domain of the enzyme, which in most lipases features the $\alpha/\beta$-hydrolase fold,[8–10] even though the sequence similarities between the various lipases is small.

Among the bacterial lipases, the 46 kDa lipase from the animal skin pathogen *Staphylococcus hyicus* (SHL) is unique in having high $A_1$ and minor $A_2$ phospholipase activities, besides having considerable lipase activity.[11,12] The enzyme was included originally in family I.5 of the bacterial lipase classification scheme proposed by Arpigny and Jaeger,[8] together with other staphylococcal lipases and thermostable lipases from *Geobacillus* species. Later, because of their lower level of sequence homology (29–37% identity) to the *Geobacillus* lipases, the *Staphylococcus* enzymes were re-assigned to family I.6.[13] Mutation studies showed that Ser124, Asp314 and His355 form the catalytic triad.[14–16] The serine residue, which is the catalytic nucleophile, is part of the typical G-X-S-X-G motif.

Since phospholipids are more polar than regular lipids, a phospholipase may be expected to have a more polar active site than a true lipase. Indeed, a mutation study of putative active site residues showed the importance of a serine residue (Ser356) next to the catalytic triad histidine residue (His355) in SHL,[17] which is a conserved, apolar residue in other staphylococcal lipases. A more elaborate study by van Kampen *et al.*, in which chimeras of SHL and the homologous *Staphylococcus aureus* lipase NCTC8530 (SAL; 53% identical and 64% similar residues; no phospholipase activity) were generated, showed that

Present addresses: M. Nardini, Department of Biomolecular Sciences and Biotechnology, University of Milano, Via Celoria 26, 20133 Milano, Italy; S. Ransac, Institut de Biochimie et Génétique Cellulaire, Université de Bordeaux-2, UMR 5095, 1 rue Camille Saint-Saëns, 33077 Bordeaux, France.

E-mail address of the corresponding author: b.w.dijkstra@rug.nl

0022-2836/$ - see front matter 

Lys295 is the major determinant of phospholipase activity and, to a lesser degree, Glu292.[17,18] In a sequence alignment, Lys295 and Glu292 align with the α9 helix of *Pseudomonas glumae* lipase (PGL) and *Pseudomonas cepacia* lipase (PCL).[19] In these lipases, this helix is located at the edge of the substrate-binding cleft, and forms the binding groove for the *sn*-1 chain of a lipid substrate,[20] which would be the binding site for the phospholipid phosphate-group in a phospholipase $A_1$ like SHL.

As well as in its phospholipase activity, SHL differs from its staphylococcal homologues and most other bacterial lipases in its broad substrate specificity.[11,21,22] Converted triacylglycerol lipid substrates may range in acyl chain length from two to 18 carbon atoms, with trioctanoylglycerol as optimal lipid substrate. Phospholipid substrates that are converted by SHL include glycerophospholipids, lysophospholipids and β-glycerophospholipids with different phospholipid head groups and acyl chain lengths of up to at least 15 carbon atoms.[11,22] Yet, the lipid and phospholipid substrates are converted with only little enantioselectivity towards the C2 position of the (phospho)lipid glycerol backbone. Some studies have attempted to explain this substrate specificity of SHL in more detail by mutation or sequence comparison with other lipases, in particular the above-mentioned homologous *S. aureus* lipase NCTC8530, which hydrolyses only short-chain triacylglycerols and acyl ester substrates.[12,18] However, chain length selectivity and enantioselectivity have been too complex to fully understand without information on the architecture of the active site.

In order to reveal the structural details of the unusual phospholipase activity of SHL, and to understand the broad substrate specificity of the enzyme, the protein was crystallized by Ransac *et al.*[23] However, due to the fragile nature of the SHL crystals, heavy-atom derivatization attempts were unsuccessful, and the structure could not be solved by anomalous dispersion or isomorphous replacement methods. Only after the structures of two homologous family I.5 members lacking phospholipase activity, the *G. stearothermophilus* lipase L1 (GSL; 36% identity)[24] and the *G. stearothermophilus* lipase P1 (GSP; 36% identity),[25] were elucidated, we were able to successfully apply molecular replacement, using a starting model based on the GSP structure. The resulting structure is presented here and shows that SHL has a binding site for the phosphate group of a phospholipid, formed by a cluster of polar amino acid residues, which explains its high level of phospholipase activity.

## Results and Discussion

### X-ray structure determination

The structure of SHL was solved by molecular replacement using a model based on the structure of the lipase from *Geobacillus stearothermophilus* P1 (GSP, PDB code 1JI3).[25] The final model contains two molecules (A and B) per asymmetric unit, related by non-crystallographic 2-fold symmetry, which are clearly defined in the electron density. The two molecules are highly similar (r.m.s.d. of 0.30 Å for 386 equivalent $C^{\alpha}$ atoms). All amino acid residues are found in the most-favoured or allowed regions of the Ramachandran plot, except for three residues in the additionally allowed region (Table 1). These are the catalytic serine residues of both molecules, and Lys36 of molecule A, which is in a poorly defined surface loop running from Thr27 to Glu38. The electron density for residue 40 indicates tyrosine and not histidine as in the original published sequence.[26] Tyrosine is absolutely conserved at this position in other family I.6 lipases; it maintains the structure of the oxyanion hole through hydrogen bonding interactions of its $O^{\eta}$ hydroxyl group with the His123 $N^{\delta}$ of the β5-α4 loop and the backbone nitrogen atom of Gly25 in the β3-α1 loop. Therefore, we conclude that the published sequence is in error at position 40.

### Overall structure

Each of the two *Staphylococcus hyicus* lipase molecules in the asymmetric unit has a heart-like shape with approximate dimensions of 60 Å × 60 Å × 50 Å. The structure is very similar to those of the two structurally characterized family I.5 members, the

**Table 1.** Data collection and refinement statistics

| | |
|---|---|
| Space group | $P2_12_12_1$ |
| Resolution (Å) | 26.71–2.86 (2.93–2.86) |
| Unit cell dimensions | |
| *a* (Å) | 73.31 |
| *b* (Å) | 77.96 |
| *c* (Å) | 169.81 |
| Completeness (%) | 98.8 (99.7) |
| $\langle I / \sigma I \rangle$ | 18.07 (8.60) |
| Average multiplicity | 6.1 |
| $R_{work}$ factor (%) | 20.7 |
| $R_{free}$ (%) | 26.3 |
| No. protein atoms | 6145 |
| No. solvent molecules | 26 |
| No. calcium ions | 2 |
| No. ions modelled as zinc | 2 |
| r.m.s. deviation from ideality | |
| Bond lengths (Å) | 0.006 |
| Bond angles (deg.) | 0.937 |
| Ramachandran plot. | |
| Residues in most-favoured and allowed regions (%) | 99.5 |
| Residues in generously allowed regions (%) | 0.4 (three residues) |
| Residues in disallowed regions | None |

| Average *B*-factors | Molecule A | Molecule B | Overall |
|---|---|---|---|
| Main chain atoms (Å$^2$) | 19.3 | 19.4 | 19.4 |
| Side-chain atoms (Å$^2$) | 19.4 | 19.5 | 19.3[a] |
| All atoms (Å$^2$) | 19.3 | 19.5 | 19.4 |

Values for the highest resolution shell are shown in brackets. $R_{work} = \sum_h ||F_{obs}| - |F_{calc}|| / \sum |F_{obs}|$, where $|F_{obs}|$ and $|F_{calc}|$ are the observed and calculated structure factor amplitudes, respectively. $R_{free}$ is calculated with 10% of the diffraction data chosen at random and not used in the refinement.

[a] For side-chain atoms and 26 water molecules.

*G. stearothermophilus* lipase P1 (GSP) and the *G. stearothermophilus* lipase L1 (GSL), and superimposes on them with an r.m.s.d. of 1.25 Å and 1.29 Å for 315 and 317 equivalent $C^{\alpha}$ atoms, respectively. SHL has an α/β-hydrolase fold,[9] with a central seven-stranded parallel β-sheet covered on one side by helices α1 and α14, and on the other side by helices α2, α4 and the short helix α13 (see Figure 1). As expected, Ser124, Asp314 and His355 form the catalytic triad. The edge of the active site is lined by helices α7, α12, and lid helices α8 and α9. As was observed in the GSP and GSL structures, the first two strands of the central β-sheet are absent compared to the canonical α/β-hydrolase topology.[9] Furthermore, the SHL topology also contains a b1-α3-b2 insertion between helix α4 and strand β5, similar to the insertion observed in the GSP and GSL structures (see Figure 2).

## SHL adopts an open conformation

In the SHL crystal structure, helices α8 (residues 190–205) and α9 (residues 226–235) are displaced by ~10 Å compared to the corresponding helices in the GSP structure (α6 and α7). As a result, there is an open, ~10 Å deep cleft in the enzyme at the active site, with the active site serine at the bottom. A normal mode analysis of this open conformation suggests that α8 and α9 move together.[27] Previously, inhibition studies have indicated the presence of a moveable lid in SHL.[14] Since the rest of the SHL and GSP structures remain closely superimposable (r.m.s.d. of 1.25 Å for 315 equivalent $C^{\alpha}$ atoms), we conclude that helices α8 and α9, and the α8-α9 loop form this flexible lid. The closed conformation of SHL is presumably very similar to that of GSP and GSL. A homology model of the closed conformation of SHL shows that the hydrophobic side of the amphipathic lid helix α8 faces the inside of the active site cavity. Yet, three important aromatic interactions made between the GSP lid helix residues Phe176, Phe180 and Phe181 and the surrounding elements, are absent from SHL.

The crystallization of SHL from a solution that contained dimethyl sulfoxide and isopropanol likely favoured the crystallization of the enzyme in the open conformation, as has been noted for other lipases crystallized from organic solvents.[28] The open conformation is stabilized by intimate hydrophobic interactions with the other molecule in the asymmetric unit. Most notably, residues Pro190, Ile192, Ile195, Leu196, Phe199, Met202 and Leu206 of helix α8 from one molecule in the asymmetric unit have van der Waals interactions with these residues from helix α8 of the neighbouring molecule. Thus, the hydrophobic residues of one α8 helix are partially covered by the α8 residues of the neighbouring molecule, and this compensates for the entropic penalty of exposing the hydrophobic residues to the solvent. Yet, this interaction between the α8 lid-helices does not occur in solution, since SHL behaves as a monomer in size-exclusion chromatography, with an apparent molecular mass of 46 kDa.[11]

## Substrate modelling and structural basis for (phospho)lipid binding

To visualise the binding of a lipid substrate in SHL, the structure of PCL with the covalently bound lipid transition state analogue $R_C$-($R_P$,$S_P$)-1,2-dioctylcarbamoylglycero-3-*O*-octylphosphonate (OCP) was superimposed on the SHL structure.[20] The ~22 Å long, ~10 Å wide and ~15 Å deep substrate-binding cleft of SHL is similar to that of PCL and has three separate binding pockets, one for each of the three lipid acyl chains (see Figure 4). Two of these pockets can hold acyl chains of about 10–14 carbon atoms. The "back" pocket (for the scissile ester acyl chain equivalent to the *sn*-3 chain of OCP; also called the HA pocket[20]), is relatively narrow with a width of ~5 Å and a length of ~12 Å. The other, the

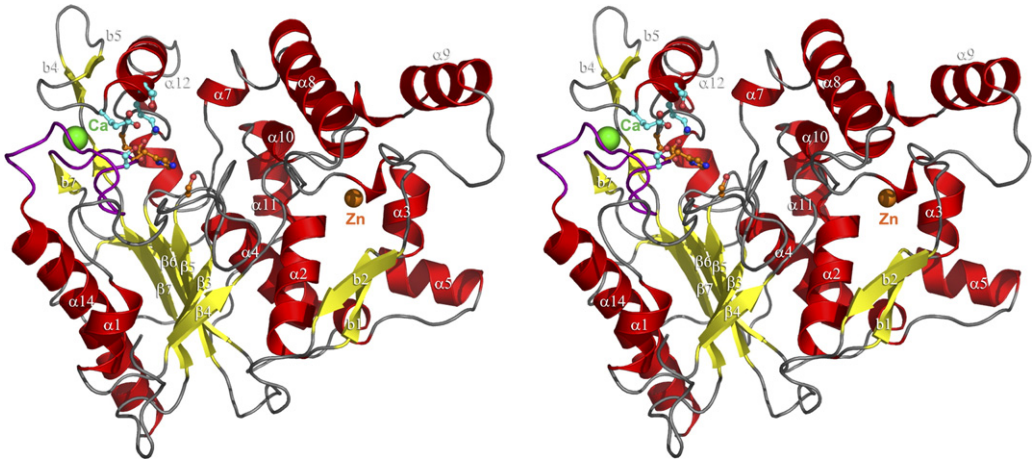


**Figure 1.** Stereo representation of the *S. hyicus* lipase structure. The calcium ion and the second ion are represented by a green sphere and an orange sphere, respectively. Residues of the catalytic triad and key residues for phospholipase activity are shown in ball-and-stick representation with carbon atoms in orange and cyan, respectively. This Figure was rendered with PyMOL [http://www.pymol.org].

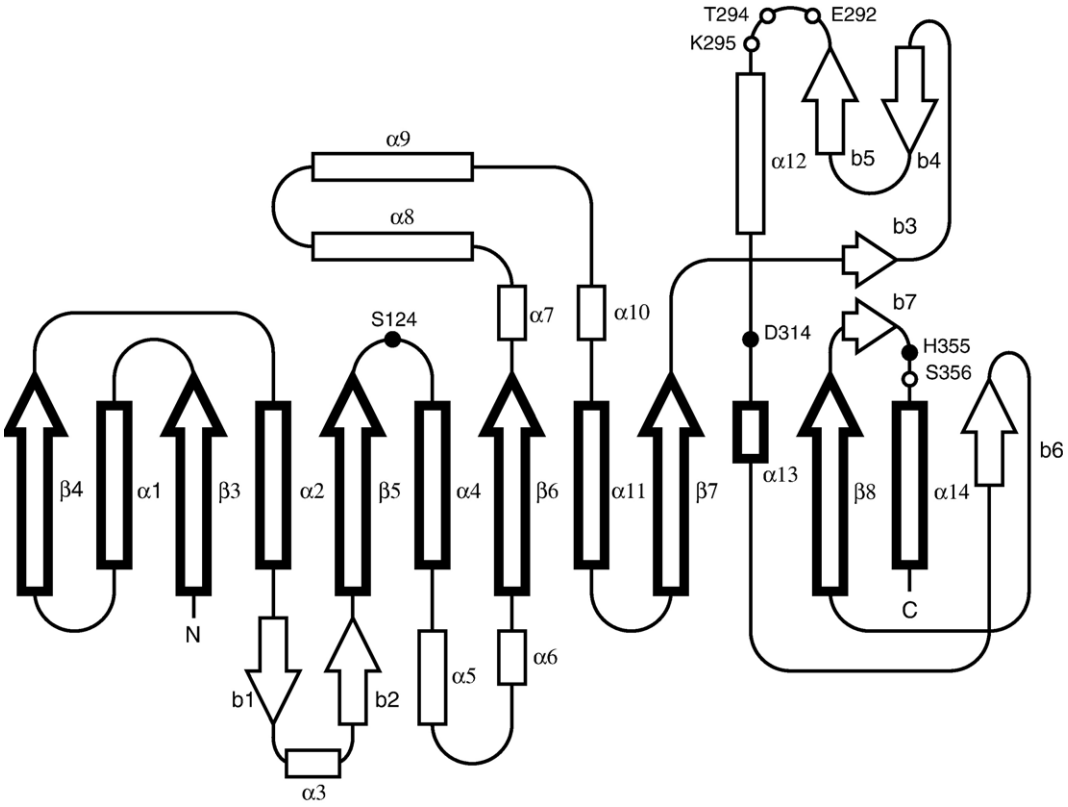


**Figure 2.** Secondary structure topology diagram of SHL. Elements of the α/β hydrolase core are indicated in bold. α-Helices and β-strands are indicated by rectangles and arrows, respectively. Residues of the catalytic triad and key residues for phospholipase activity in SHL are indicated with filled and open circles, respectively. SHL, GSP and GSL have a large insertion between helix α2 and strand β5, corresponding to helix αB and strand β5 of the canonical α/β-hydrolase fold. The nomenclature of β-strands is according to the canonical α?β-hydrolase fold.[9] The first N-terminal β-strand corresponds to β3 of the canonical α/β-hydrolase fold.

spacious "front" pocket (for the *sn*-2 acyl chain of OCP; the HH pocket[20]), resembles a funnel expanding outwards, starting with a width of ~7.5 Å at the ester carbonyl atom of the acyl chain. The back and front pockets are lined by mostly hydrophobic residues that can make van der Waals interactions with the acyl chains of the substrate.

In contrast, the "middle" pocket (for the *sn*-1 acyl chain of OCP; the HB pocket[20]) can accommodate an acyl chain of up to about six carbon atoms only without the acyl chain protruding into the solvent. One of its walls contains four polar residues (Glu292, Thr294, Lys295 and Ser356), which form a cluster with Lys295 at the centre. Glu292, Thr294 and Ser356 bind the positively charged $N^{\zeta}$ group of Lys295 and keep the Lys295 side-chain in position. Its $N^{\zeta}$ group is about 3.5 Å from the *sn*-1 carbonyl group of the modelled OCP. Beyond the polar cluster, the residues are hydrophobic and may thus be able to interact with the rest of the acyl chain through van der Waals interactions. Alternatively, since the opposite wall of the wide middle pocket is mostly hydrophobic (see Figure 4), the acyl chain may also bind to that wall.

To investigate phospholipid binding to SHL, the readily hydrolysed substrates 1,2-dioctanoyl-*sn*-glycero-3-phosphocholine (L-di$C_8$PC) and 2,3-dioctanoyl-*sn*-glycero-1-phosphocholine (D-di$C_8$PC) were modelled in the tetrahedral transition state in the active site of SHL, using the binding mode of OCP as a guide. Their phosphate groups take a position equivalent to that of the *sn*-1 carbonyl group of OCP. Lys295 is thus correctly positioned to bind the carbonyl oxygen atom of a lipid substrate, and it can bind the phosphate group of a phospholipid. These observations closely match the results of previous studies,[17,18,29] which implicated Ser356 and residues in the 290–297 range in phospholipid binding.[17] In particular, Lys295 appeared to be a major determinant of phospholipase activity, with a somewhat lesser role for Glu292.[18] Although the Lys295–Glu292 salt-bridge (2.5 Å) may seem the key contribution to keep the Lys295 side-chain in position, mutation of the glutamate was found to have only a minor effect on the phospholipase activity of the enzyme, while the Ser356Val mutation had a much larger effect.[17,18] Ser356 anchors the N terminus of the α12 helix to the b7-α14 loop, and is thus important for keeping the other polar cluster residues in place, which may explain why mutation of Ser356 has a much larger negative effect than mutation of Glu292. Our model also explains why SHL has little preference for the two stereo configurations at the C2 position.[22] As depicted in Figure 5, the space afforded by the wide middle binding pocket allows both enantiomers to bind produc-

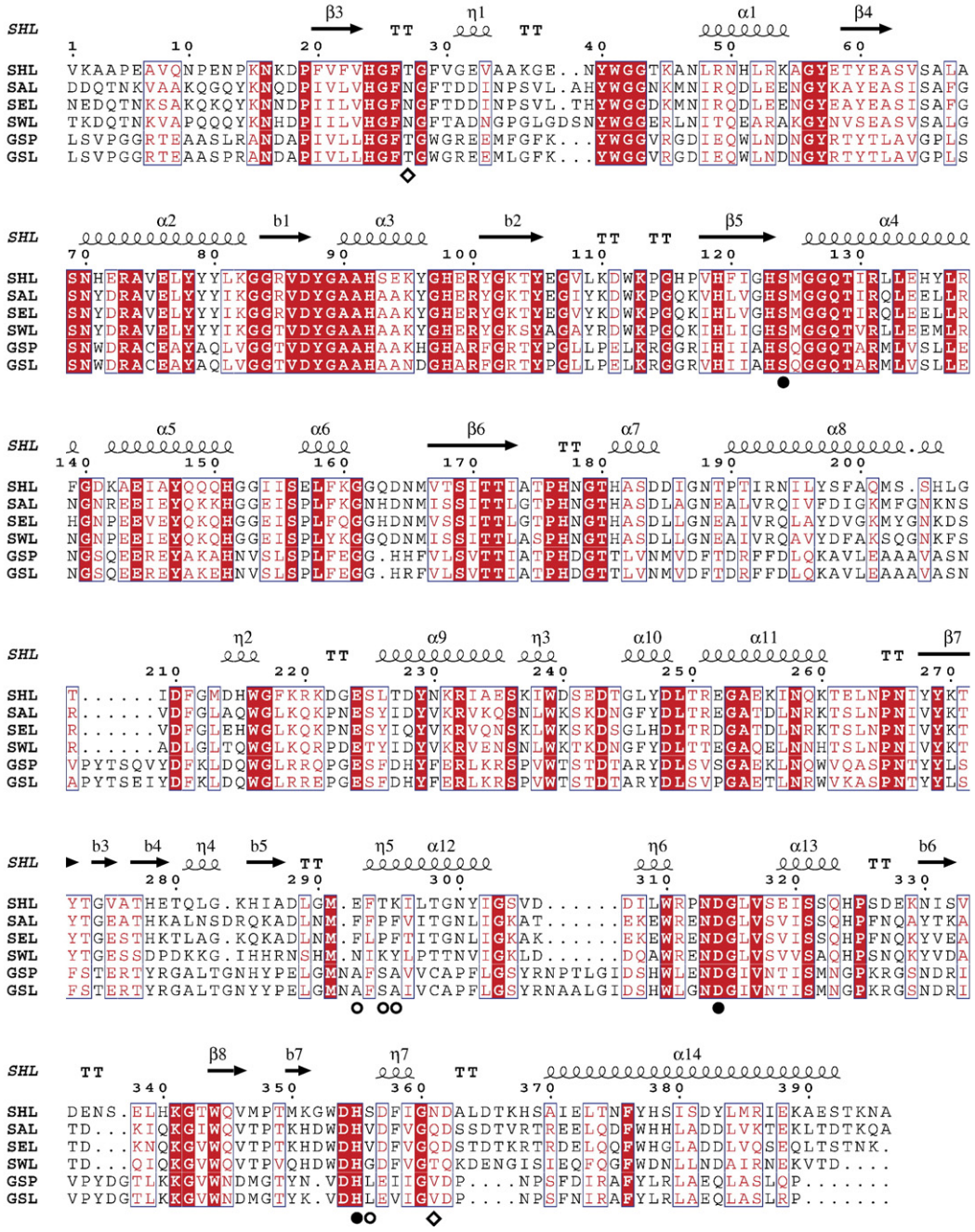


**Figure 3.** Structure-based sequence alignment of *S. hyicus* lipase (SHL), *S. aureus* NCTC8530 lipase (SAL), *S. epidermidis* RP62A lipase (SEL), *S. warneri* 863 lipase (SWL), *G. stearothermophilus* lipase P1 (GSP) and *G. stearothermophilus* lipase L1 (GSL). Secondary structure elements of SHL are indicated above the sequences. Conserved residues are shown as red characters in boxes with blue lines; identical residues are shown as white characters on a red background. The residues that form the catalytic triad and those that form the polar cluster involved in phospholipid head group binding in SHL are marked under the sequences with filled and open circles, respectively. The positions of the front pocket residues Thr27 and Asn361 are marked with open diamonds. The alignment was generated with ESPript.[45]

tively, with their phosphate groups interacting with the Lys295 $N^{\zeta}$ group.

Finally, our structure suggests an explanation for the finding that SHL does not show interfacial activation with phospholipid substrates, while it does with lipids.[11] A model of the closed conformation of SHL, based on the structure of GSP, shows that the side-chain of Thr294, one of the residues of the polar cluster that binds the phospholipid head group, interacts with Ser198 of lid helix α8. Thr294 and Ser198 are located at the surface of the molecule, at the edge of the substrate-binding site. When a phospholipid substrate binds with its phosphate group to the polar cluster, it may disrupt the Thr294–Ser198 interaction, resulting in lid opening even in the absence of a lipid–water interface. Lipid

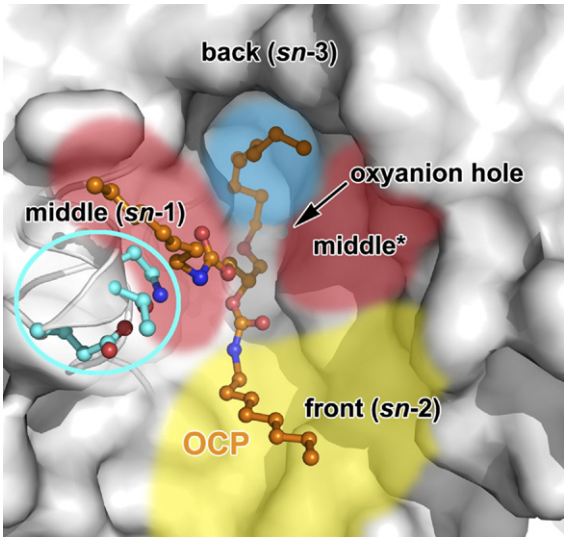


**Figure 4.** Overview of the three acyl chain binding pockets of the substrate-binding site in SHL and a model of the bound $R_C$-($R_P$,$S_P$)-1,2-dioctylcarbamoylglycero-3-*O*-octylphosphonate (OCP) lipid analogue (indicated with carbon atoms in orange). The positions of the "back", "middle" and "front" acyl binding pockets are indicated by blue, red and yellow shading, respectively. The OCP lipid analogue interacts with one wall of the middle binding pocket, while the opposite wall of the middle pocket (indicated with middle*) is exposed to the solvent. Three of the four polar residues that line the polar middle pocket wall, Glu292, Thr294 and Lys295, are shown with carbon atoms in cyan and highlighted with a cyan circle; the fourth polar residue, Ser356, has been omitted for clarity. The Figure was rendered with PyMOL [http://www.pymol.org].

substrates do not bind to the polar cluster and the Thr294–Ser198 interaction remains intact. The lid opens only in the presence of lipid aggregates, exposing its apolar side to the lipid aggregates. The resulting opening of the active site allows the substrate to enter and results in increased activity.

### Substrate size tolerance and enantioselectivity

To understand why SHL is able to hydrolyse medium-chain and long-chain triacylglycerol substrates, we compared its amino acid sequence to those of the close homologues *S. aureus* NCTC8530 lipase (SAL),[22] *S. epidermidis* lipase RP62A (SEL)[30] and *S. warneri* lipase 863 (SWL),[31] which hydrolyse only short triacylglycerols with chain lengths of up to eight (SAL, SEL) or 12 (SWL) carbon atoms (see Figure 3). Since no structure of SAL, SEL or SWL is available, we generated models of these staphylococcal lipases on the basis of the SHL structure.[32] A comparison of sequences and structures showed that residues of the back pocket are highly conserved and the volumes are virtually the same. In the middle pocket, several residues differ among the staphylococcal lipases, but since the middle pocket is only shallow, we believe these substitutions cannot explain the differences in substrate specificity between the compared lipases. In contrast, the front pocket of SHL is larger and capable of making more interactions with the *sn*-2 acyl chain of the substrate, and there is variability among several of the front pocket residues, most notably Thr27 (Thr/Asn) and Asn361 (Asn/Gln/Thr/Val). Strikingly, the equivalent of Thr27 is asparagine in the lipases that prefer

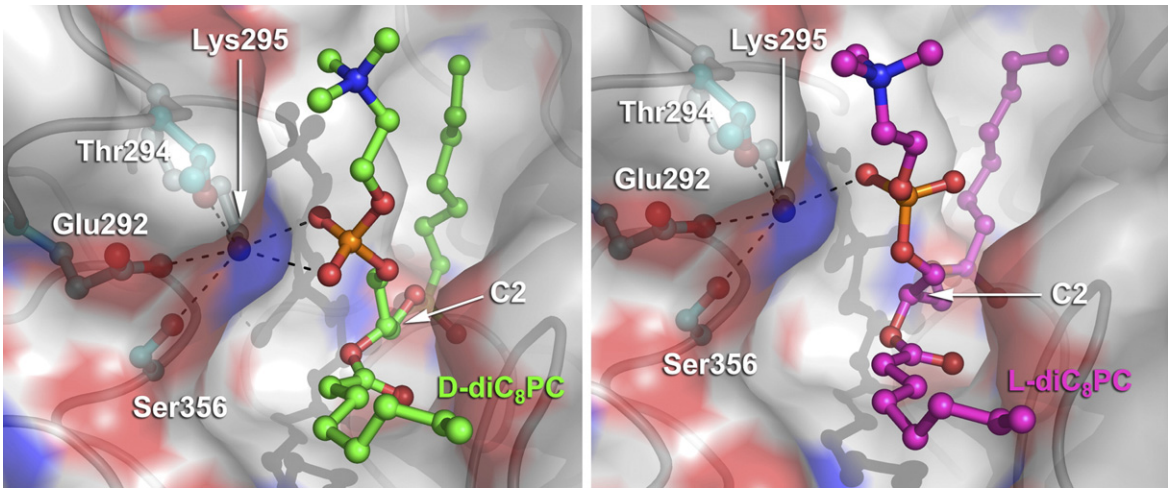


**Figure 5.** Models of D-diC$_8$PC (left picture) and L-diC$_8$PC (right picture) bound in the active site of *S. hyicus* lipase, generated on the basis of the structure of *P. cepacia* lipase in complex with the inhibitor $R_C$-($R_P$,$S_P$)-1,2-dioctylcarbamoylglycero-3-*O*-octylphosphonate. Lys295, Glu292, Thr294 and Ser356, the determinants of SHL phospholipase activity, are depicted with carbon atoms in cyan. The modelled D-diC$_8$PC and L-diC$_8$PC substrates are shown with green and purple carbon atoms, respectively. The C2 carbon stereo-centre of the phospholipid glycerol backbone is indicated. Electrostatic interactions between the side-chain of Lys295 and surrounding residues, as well as with the substrate phosphate oxygen atoms are shown as black dashes. SHL is shown in a transparent surface representation, which is coloured red and blue at the oxygen and nitrogen positions, respectively. This Figure was rendered with PyMOL [http://www.pymol.org].

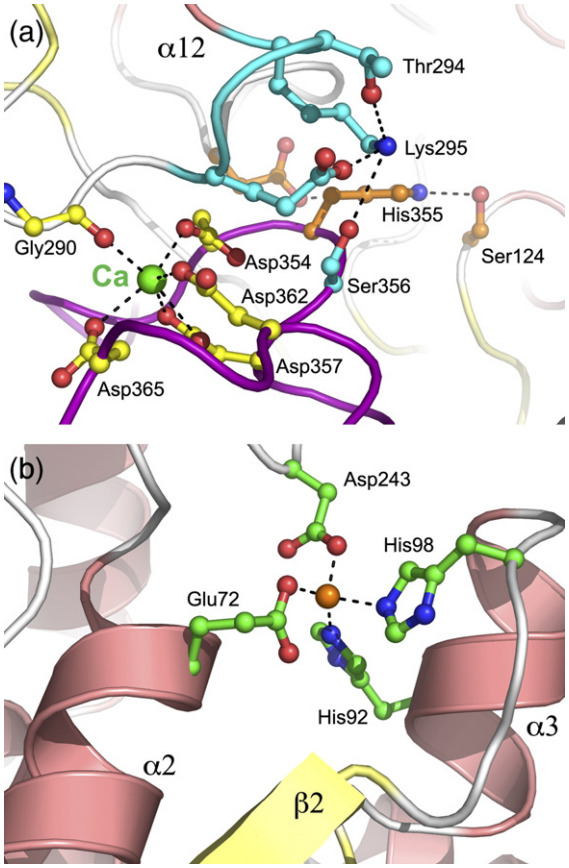


**Figure 6.** (a) The calcium ion (shown in green) connecting Asp354, Asp357, Asp362, and Asp365 of the b7-α14 loop (indicated in purple) to Gly290, which is part of the b5-α12 loop. Calcium-binding residues are shown with carbon atoms in yellow, residues of the catalytic triad are shown with carbon atoms in orange. The α12 helix and carbon atoms of the phospholipid head group binding residues are coloured cyan. (b) Tetrahedral coordination of the second ion by Glu72, His92, His98 and Asp243. The ligating residues are shown with carbon atoms in green, the ion is shown in orange. This Figure was rendered with PyMOL [http://www.pymol.org].

short-chain substrates. Analogous to PCL,[20] Thr27 in SHL may donate a hydrogen bond to the *sn*-2 carbonyl oxygen atom of the substrate, thus providing an important protein–substrate interaction. Therefore, a change from threonine to asparagine may have consequences for substrate binding and substrate specificity. Further (mutation) studies are necessary to pinpoint the roles of Thr27 and Asn361 in substrate specificity. It should be noted, though, that normal mode analysis and structure comparison of SHL, GSP, GSL, PCL and PAL shows that part of the front pocket is flexible.[27] This flexibility and the variability among the front pocket residues, and the absence of crystal structures of lipases with a preference for short-chain substrates, preclude, at this moment, a more detailed explanation of the determinants of the chain-length specificity of family I.6 lipases.

## Ion binding and contribution to stability

Two cations, a calcium ion and probably a zinc ion, are present in SHL, in similar positions to the bound metal ions in the structures of *G. stearothermophilus* lipase P1 and lipase L1. Various studies have shown that SHL binds calcium. Removal of this ion drastically reduced the activity to ~2.5-5% of that of the holo-enzyme.[22,30] This significant residual activity, along with the observation that calcium protects SHL against unfolding by urea,[21] indicates that the calcium is not involved directly in stabilizing the oxyanion transition state, as in phospholipases $A_2$,[33,34] but rather has a structural role, as observed in the structures of the *Pseudomonas*[28,35] and *G. stearothermophilus*[24] lipases.

Mutation studies had already indicated the importance of the side-chains of Asp354 and Asp357 for calcium binding.[19] Our SHL structure shows that these two residues are a monodentate and a bidentate calcium binding ligand, respectively (Figure 6(a)). In addition to these residues, one carboxylate oxygen atom each of Asp362 and Asp365, and the backbone carbonyl oxygen atom of Gly290 are monodentate ligands of the calcium. These ligands ligate the calcium ion with a distorted octahedral geometry, with binding distances of 2.4–2.7 Å. Due to its position, 10–15 Å away from the catalytic triad and 9 Å away from Lys295, it is clear that the calcium is not involved directly in the (phospho)lipase reaction or in binding the phosphate moiety of a phospholipid.

The stabilizing role of calcium can now be understood. Calcium stabilizes the conformation of the b7-α14 loop, since it interconnects residues Asp354, Asp357, Asp362 and Asp365 in this loop. Furthermore, the calcium also connects, *via* Gly290, the b7-α14 loop to the N terminus of helix α12. Both the stabilization of the b7-α14 loop and that of the N terminus of helix α12 are important for the catalytic activity of SHL. The b7-α14 loop contains His355, which is part of the catalytic triad, and Ser356, which is important for phospholipid head group binding; the N terminus of helix α12 contains the other polar residues Glu292, Thr294 and Lys295 involved in phospholipid head group binding. Since the calcium is important for the stabilization of the catalytic triad, as in the *Pseudomonas* and *G. stearothermophilus* lipases, and maintains the phospholipid head group-binding cluster, the loss of calcium binding may have a more profound effect on the phospholipase activity of SHL than on its lipase activity.

A second ion with tetrahedral coordination is bound by the side-chains of residues Glu72, His92, His98 and Asp243 with binding distances of 1.9–2.3 Å (Figure 6(b)). These residues are conserved in the GSP and GSL lipases as well, where they were shown to bind a zinc ion.[24,25] In the GSP and GSL lipases, zinc enhances the stability of the enzyme.[36] Such a stabilizing role in SHL can be envisaged, since the ion keeps together different parts of the peptide chain, i.e. the secondary structure elements helix α3, loop α3-b2, helix α2, and loop α9-α10 are interconnected by the

ion through residues His92, His98, Glu72 and Asp243, respectively.

### Concluding remarks

The *S. hyicus* lipase is the first lipase family I.6 member of which a 3D-structure has been elucidated. The structure closely resembles that of two Geobacillus lipases from lipase family I.5, GSL and GSP, demonstrating the little difference between the two lipase families. However, in contrast to GSL and GSP, SHL was crystallized in an open conformation. The open conformation of SHL allowed us to model the binding of a lipid substrate, as well as the two C2 enantiomers of a phospholipid substrate. Aided by these substrate-binding models, two prominent features of the middle and front pockets of the substrate-binding site were identified, that may account for the enzyme's distinctive activity compared to its close homologues from other *Staphylococcus* species and *G. stearothermophilus*. Firstly, the middle binding pocket is remarkably polar at one side, due to the presence of four hydrophilic residues, Glu292, Thr294, Lys295 and Ser356. Modelling showed that the lysine is in a good position to bind the phosphate group of a phospholipid substrate, thus explaining the high $A_1$ phospholipase activity of SHL. Secondly, the lack of enantioselectivity of SHL may be explained by the wide middle binding pocket, which allows the bonding of either glycerol C2 enantiomer. Furthermore, the tolerance of SHL towards substrate size may be explained by the acyl chain binding in the front pocket, which displays both sequence variation as well as conformational plasticity among the lipases. Most notably, Thr27, which provides an important enzyme–substrate interaction, is asparagine in staphylococcal lipases with a preference for short-chain lipids.

## Material and Methods

### Expression, purification, crystallization and data collection for *S. hyicus* lipase

The expression of SHL in *Escherichia coli* and purification has been described.[11,14] The SHL produced in *E. coli* is 35 amino acid residues longer than the native (mature) enzyme due to the cloning procedure,[14] but the specific activity of this 48 kDa expression product is the same as that of the wild-type enzyme. Its successful crystallization and data collection were reported by Ransac *et al.*[23] Briefly, 15 μl drops of 8.7 mg/ml of protein dissolved in low-salt buffer (13 mM NaCl in 1.6 mM Na succinate, pH 6.5) were equilibrated for several months at 4 °C against a reservoir containing 18–24% (v/v) DMSO and 10% (v/v) isopropanol. The fragile crystals diffracted to 2.86 Å resolution, and have $P2_12_12_1$ space group symmetry with unit cell dimensions $a=73.31$ Å, $b=77.96$ Å, $c=169.81$ Å. With two molecules of 48 kDa in the asymmetric unit, the $V_M$ is thus 2.5 $Å^3$ $Da^{-1}$ (51% (v/v) solvent content). Diffraction data was collected at 277 K at the X31 beamline of the EMBL outstation at the DESY synchrotron in Hamburg.[9] The MOSFLM,[37] ROTAVATA, AGROVATA and TRUNCATE programs of the CCP4 package were used for integration, scaling and merging of the data.[38] Details of the data collection and refinement statistics are given in Table 1.

### Structure determination, refinement and analysis

The structure of SHL was solved by molecular replacement using the program AMoRe with a starting model based on the structure of *G. stearothermophilus* lipase P1. The starting model included residues 16–180 and 235–365 of GSP, thus excluding the residues of the lid domain. All residues that differed in SHL were changed to alanine. The initial solution from AMoRE was improved by rigid body refinement and non-crystallographic symmetry restrained refinement in CNS.[39] Application of the program Resolve with the prime-and-switch option resulted in electron density maps that were clear enough to trace most residues in the sequence.[40] Successive rounds of positional and individual *B*-factor refinement using CNS and Refmac,[41] yielded $R_{work}$ and $R_{free}$ factors of 20.7% and 26.3% with a final model that included 387 and 386 out of a total of 431 residues for molecules A and B, respectively, as well as two ions in each molecule, together with a total of 26 water molecules. The 35 residues that were present at the N terminus of SHL due to the cloning procedure in *E. coli* were not visible in the electron density. Secondary structure assignments were made with DSSP.[42]

### Structural alignment and modelling

The structures of SHL in complex with the covalently bound L-di$C_8$PC and D-di$C_8$PC in the tetrahedral transition state were manually modelled on the basis of the PCL OCP complex structure.[20] As a reference for manual modelling, the OCP lipid substrate analogue was placed in the active site of SHL by superposition of the PCL enzyme-substrate analogue onto that of SHL, with an r.m.s.d. of 1.20 Å for 182 equivalent $C^\alpha$ atoms. The L-di$C_8$PC and D-di$C_8$PC were manually placed in the active site of SHL in Coot,[43] using constraints that were generated using the PRODRG webserver.[44] Models of SAL, SEL and SWL were generated using the SWISS-MODEL server on the basis of the coordinates of SHL.[32]

### Protein Data Bank accession code

The atomic coordinates and structure factors for the SHL structure have been deposited in the Protein Data Bank with accession code 2HIH.

## Acknowledgements

We thank H. J. Rozeboom for help with structure refinement. All members of the Groningen protein crystallography group are thanked for helpful discussions. This work was supported by the Netherlands Organisation for Scientific Research (NWO).

## References

1. Jaeger, K. E., Dijkstra, B. W. & Reetz, M. T. (1999). Bacterial biocatalysts: molecular biology, three-dimensional structures, and biotechnological applications of lipases. *Annu. Rev. Microbiol.* **53**, 315–351.

2. Götz, F., Verheij, H. M. & Rosenstein, R. (1998). Staphylococcal lipases: molecular characterisation, secretion, and processing. *Chem. Phys. Lipids*, **93**, 15–25.
3. Rosenstein, R. & Götz, F. (2000). Staphylococcal lipases: biochemical and molecular characterization. *Biochimie*, **82**, 1005–1014.
4. Gupta, R., Gupta, N. & Rathi, P. (2004). Bacterial lipases: an overview of production, purification and biochemical properties. *Appl. Microbiol. Biotechnol.* **64**, 763–781.
5. Sarda, L. & Desnuelle, P. (1958). Actions of pancreatic lipase on esters in emulsions. *Biochim. Biophys. Acta*, **30**, 513–521.
6. Derewenda, Z. S. & Sharp, A. M. (1993). News from the interface: the molecular structures of triacylglyceride lipases. *Trends Biochem. Sci.* **18**, 20–25.
7. Secundo, F., Carrea, G., Tarabiono, C., Gatti-Lafranconi, P., Brocca, S., Lotti, M. *et al.* (2006). The lid is a structural and functional determinant of lipase activity and selectivity. *J. Mol. Cat. B Enzym.* **39**, 166–170.
8. Arpigny, J. L. & Jaeger, K. E. (1999). Bacterial lipolytic enzymes: classification and properties. *Biochem. J.* **343**, 177–183.
9. Nardini, M. & Dijkstra, B. W. (1999). $\alpha/\beta$ Hydrolase fold enzymes: the family keeps growing. *Curr. Opin. Struct. Biol.* **9**, 732–737.
10. Ollis, D. L., Cheah, E., Cygler, M., Dijkstra, B., Frolow, F., Franken, S. M. *et al.* (1992). The $\alpha/\beta$ hydrolase fold. *Protein Eng.* **5**, 197–211.
11. van Oort, M. G., Deveer, A. M. T. J., Dijkman, R., Leuveling Tjeenk, M., Verheij, H. M., de Haas, G. H. *et al.* (1989). Purification and substrate specificity of *Staphylococcus hyicus* lipase. *Biochemistry*, **28**, 9278–9285.
12. Simons, J. W. F. A., Götz, F., Egmond, M. R. & Verheij, H. M. (1998). Biochemical properties of staphylococcal (phospho)lipases. *Chem. Phys. Lipids*, **93**, 27–37.
13. Jaeger, K. E. & Eggert, T. (2002). Lipases for biotechnology. *Curr. Opin. Biotechnol.* **13**, 390–397.
14. Leuveling Tjeenk, M., Bulsink, Y. B. M., Slotboom, A. J., Verheij, H. M., de Haas, G. H., Demleitner, G. & Götz, F. (1994). Inactivation of *Staphylococcus hyicus* lipase by hexadecylsulfonyl fluoride: evidence for an active site serine. *Protein Eng.* **7**, 579–583.
15. Jäger, S., Demleitner, G. & Götz, F. (1992). Lipase of *Staphylococcus hyicus*: analysis of the catalytic triad by site-directed mutagenesis. *FEMS Microbiol. Letters*, **100**, 249–254.
16. Boots, J. W. P., van Dongen, W. D., Verheij, H. M., de Haas, G. H., Haverkamp, J. & Slotboom, A. J. (1995). Identification of the active site histidine in *Staphylococcus hyicus* lipase using chemical modification and mass spectrometry. *Biochim. Biophys. Acta*, **1248**, 27–34.
17. van Kampen, M. D., Simons, J. W. F. A., Dekker, N., Egmond, M. R. & Verheij, H. M. (1998). The phospholipase activity of *Staphylococcus hyicus* lipase strongly depends on a single Ser to Val mutation. *Chem. Phys. Lipids*, **93**, 39–45.
18. van Kampen, M. D., Verheij, H. M. & Egmond, M. R. (1999). Modifying the substrate specificity of staphylococcal lipases. *Biochemistry*, **38**, 9524–9532.
19. Simons, J. W. F. A., van Kampen, M. D., Ubarretxena-Belandia, I., Cox, R. C., Alves dos Santos, C. M., Egmond, M. R. & Verheij, H. M. (1999). Identification of a calcium binding site in *Staphylococcus hyicus* lipase: generation of calcium-independent variants. *Biochemistry*, **38**, 2–10.
20. Lang, D. A., Mannesse, M. L. M., de Haas, G. H., Verheij, H. M. & Dijkstra, B. W. (1998). Structural basis of the chiral selectivity of *Pseudomonas cepacia* lipase. *Eur. J. Biochem.* **254**, 333–340.
21. Simons, J. W. F. A., Boots, J. W., Kats, M. P., Slotboom, A. J., Egmond, M. R. & Verheij, H. M. (1997). Dissecting the catalytic mechanism of staphylococcal lipases using carbamate substrates: chain length selectivity, interfacial activation, and cofactor dependence. *Biochemistry*, **36**, 14539–14550.
22. Simons, J. W. F. A., Adams, H., Cox, R. C., Dekker, N., Götz, F., Slotboom, A. J. & Verheij, H. M. (1996). The lipase from *Staphylococcus aureus*. Expression in *Escherichia coli*, large-scale purification and comparison of substrate specificity to *Staphylococcus hyicus* lipase. *Eur. J. Biochem.* **242**, 760–769.
23. Ransac, S., Blaauw, M., Dijkstra, B. W., Slotboom, A. T., Boots, J. W. P. & Verheij, H. M. (1995). Crystallization and preliminary X-ray analysis of a lipase from *Staphylococcus hyicus*. *J. Struct. Biol.* **114**, 153–155.
24. Jeong, S. T., Kim, H. K., Kim, S. J., Chi, S. W., Pan, J. G., Oh, T. K. & Ryu, S. E. (2002). Novel zinc-binding center and a temperature switch in the *Bacillus stearothermophilus* L1 lipase. *J. Biol. Chem.* **277**, 17041–17047.
25. Tyndall, J. D., Sinchaikul, S., Fothergill-Gilmore, L. A., Taylor, P. & Walkinshaw, M. D. (2002). Crystal structure of a thermostable lipase from *Bacillus stearothermophilus* P1. *J. Mol. Biol.* **323**, 859–869.
26. Götz, F., Popp, F., Korn, E. & Schleifer, K. H. (1985). Complete nucleotide sequence of the lipase gene from *Staphylococcus hyicus* cloned in *Staphylococcus carnosus*. *Nucl. Acids Res.* **13**, 5895–5906.
27. Suhre, K. & Sanejouand, Y. H. (2004). On the potential of normal-mode analysis for solving difficult molecular-replacement problems. *Acta Crystallog. sect. D*, **60**, 796–799.
28. Kim, K. K., Song, H. K., Shin, D. H., Hwang, K. Y. & Suh, S. W. (1997). The crystal structure of a triacylglycerol lipase from *Pseudomonas cepacia* reveals a highly open conformation in the absence of a bound inhibitor. *Structure*, **5**, 173–185.
29. van Kampen, M. D., Dekker, N., Egmond, M. R. & Verheij, H. M. (1998). Substrate specificity of *Staphylococcus hyicus* lipase and *Staphylococcus aureus* lipase as studied by in vivo chimeragenesis. *Biochemistry*, **37**, 3459–3466.
30. Simons, J. W. F. A., van Kampen, M. D., Riel, S., Götz, F., Egmond, M. R. & Verheij, H. M. (1998). Cloning, purification and characterisation of the lipase from *Staphylococcus epidermidis* - comparison of the substrate selectivity with those of other microbial lipases. *Eur. J. Biochem.* **253**, 675–683.
31. van Kampen, M. D., Rosenstein, R., Götz, F. & Egmond, M. R. (2001). Cloning, purification and characterisation of *Staphylococcus warneri* lipase 2. *Biochim. Biophys. Acta*, **1544**, 229–241.
32. Schwede, T., Kopp, J., Guex, N. & Peitsch, M. C. (2003). SWISS-MODEL: an automated protein homology-modeling server. *Nucl. Acids Res.* **31**, 3381–3385.
33. Thunnissen, M. M. G. M., Ab, E., Kalk, K. H., Drenth, J., Dijkstra, B. W., Kuipers, O. P. *et al.* (1990). X-ray structure of phospholipase $A_2$ complexed with a substrate-derived inhibitor. *Nature*, **347**, 689–691.
34. Scott, D. L., White, S. P., Browning, J. L., Rosa, J. J., Gelb, M. H. & Sigler, P. B. (1991). Structures of free and inhibited human secretory phospholipase $A_2$ from inflammatory exudate. *Science*, **254**, 1007–1010.
35. Nardini, M., Lang, D. A., Liebeton, K., Jaeger, K. E. & Dijkstra, B. W. (2000). Crystal structure of *Pseudomonas aeruginosa* lipase in the open conformation. The pro-

totype for family I.1 of bacterial lipases. *J. Biol. Chem.* **275**, 31219–31225.
36. Choi, W. C., Kim, M. H., Ro, H. S., Ryu, S. R., Oh, T. K. & Lee, J. K. (2005). Zinc in lipase L1 from *Geobacillus stearothermophilus* L1 and structural implications on thermal stability. *FEBS Letters*, **579**, 3461–3466.
37. Leslie, A. G. (2006). The integration of macromolecular diffraction data. *Acta Crystallog. sect. D*, **62**, 48–57.
38. Collaborative Computing Project Number 4. (1994). The CCP4 suite: programs for protein crystallography. *Acta Crystallog. sect. D*, **50**, 760–763.
39. Brünger, A. T., Adams, P. D., Clore, G. M., DeLano, W. L., Gros, P., Grosse-Kunstleve, R. W. *et al.* (1998). Crystallography & NMR system: a new software suite for macromolecular structure determination. *Acta Crystallog. sect. D*, **54**, 905–921.
40. Terwilliger, T. C. (2001). Map-likelihood phasing. *Acta Crystallog. sect D*, **57**, 1763–1775.
41. Murshudov, G. N., Vagin, A. A. & Dodson, E. J. (1997). Refinement of macromolecular structures by the maximum-likelihood method. *Acta Crystallog. sect. D*, **53**, 240–255.
42. Kabsch, W. & Sander, C. (1983). Dictionary of protein secondary structure: pattern recognition of hydrogen-bonded and geometrical features. *Biopolymers*, **22**, 2577–2637.
43. Emsley, P. & Cowtan, K. (2004). Coot: model-building tools for molecular graphics. *Acta Crystallog. sect. D*, **60**, 2126–2132.
44. Schüttelkopf, A. W. & van Aalten, D. M. F. (2004). PRODRG: a tool for high-throughput crystallography of protein-ligand complexes. *Acta Crystallog. sect. D*, **60**, 1355–1363.
45. Gouet, P., Courcelle, E., Stuart, D. I. & Métoz, F. (1999). ESPript: analysis of multiple sequence alignments in PostScript. *Bioinformatics*, **15**, 305–308.

***Edited by R. Huber***

*(Received 15 March 2007; received in revised form 11 May 2007; accepted 15 May 2007)*
Available online 21 May 2007